

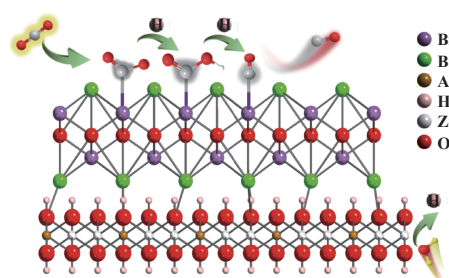
### Unveiling the Interfacial Charge Migration and Activity Origin of Heterojuncted BiOBr/ZnAl-LDH for Photocatalytic CO<sub>2</sub> Reduction

WANG Zhengchao, HUANG Xiaojuan, BI Yingpu, ZHANG Yajun

J. Mol. Catal. (China) **2025**, 39(2): 101–110.

This study presents the development of a BiOBr/ZnAl-LDH heterostructured photocatalyst *via* electrostatic self-assembly for efficient photocatalytic CO<sub>2</sub> reduction. The structural and chemical properties of the composite were systematically investigated using advanced characterization techniques, including *in-situ* X-ray diffraction (IS-XRD) and *in-situ* X-ray photoelectron spectroscopy (IS-XPS). The BiOBr/ZnAl-LDH heterostructure demonstrated a significantly enhanced CO evolution rate of 46.03  $\mu\text{mol}\cdot\text{g}^{-1}\cdot\text{h}^{-1}$  under simulated solar irradiation, surpassing the performance of pristine ZnAl-LDH (6.88  $\mu\text{mol}\cdot\text{g}^{-1}\cdot\text{h}^{-1}$ ) and BiOBr (21.58  $\mu\text{mol}\cdot\text{g}^{-1}\cdot\text{h}^{-1}$ ). Key mechanistic insights were elucidated through IS-XPS and IS-DRIFTS analyses, revealing dynamic interfacial charge transfer and surface chemical state evolution

during the reaction. CO<sub>2</sub> molecules were preferentially adsorbed on Bi sites in BiOBr, forming Bi-bound Bi—\*CO<sub>2</sub> and Bi—\*CO intermediates, while H<sub>2</sub>O oxidation occurred at Zn sites in ZnAl-LDH, supplying protons for CO<sub>2</sub> reduction. *In-situ* XRD and DRIFTS further revealed lattice expansion/contraction and intermediate species (\*COOH, \*CO) during the reaction, highlighting the critical role of interfacial interactions. The work emphasizes the synergy between BiOBr and ZnAl-LDH in optimizing charge dynamics and surface reactivity, providing a framework for designing heterostructured photocatalysts for sustainable CO<sub>2</sub> conversion. This study not only advances the mechanistic understanding of interfacial processes in photocatalytic systems but also offers practical strategies for engineering high-performance materials for solar-driven environmental and energy applications.



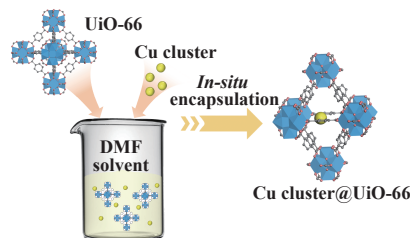
### Cu Cluster@UiO-66 Cluster-loaded Catalysts for Photocatalytic CO<sub>2</sub> Hydrogenation Reaction

WANG Xiulin, QI Shaopeng, ZHOU Kun, DENG Xi, YAO Huichao, DAI Ruoyun, ZHANG Yuqing, WU Sida, NIE Suofu

J. Mol. Catal. (China) **2025**, 39(2): 111–119.

Aiming at the stability of highly active Cu-based cluster catalysts, we constructed the Cu cluster@UiO-66 composite by using the unique structural confinement effect of MOFs to anchor the Cu in UiO-66 can not only act as a light-absorbing unit to capture sunlight to form photogenerated carriers, but also provide the porous structural stability on the microscopic scale. It is found that during the photocatalytic reaction, the

photogenerated electrons of UiO-66 can be rapidly transferred to the Cu cluster, which serves as the catalytically active site to drive the CO<sub>2</sub> reduction reaction. The photocatalytic CO<sub>2</sub> hydrogenation reaction activity is significantly enhanced, benefiting from the efficient charge transfer and stable cluster active site structure in the composite. The related research results provide a new idea for the synthesis of MOFs-supported cluster materials.



### Novel Catalyst Based on MOFs for Photocatalytic Conversion of CO<sub>2</sub> to Formic Acid

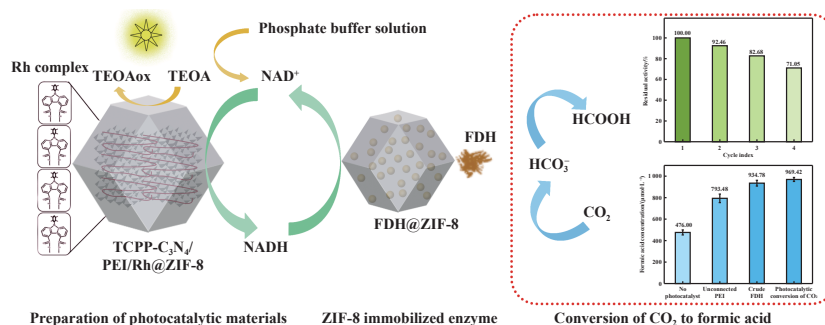
CHEN Min, WU Siyi, ZHONG Haojie, HU Jiahuan, FU Yongqian, SUN Xiaolong

J. Mol. Catal. (China) **2025**, 39(2): 120–128.

We have prepared two types of catalysts utilizing metal-organic frameworks: One is a self-prepared photocatalytic material, TCPP-C<sub>3</sub>N<sub>4</sub>/PEI/Rh, encapsulated within the metal-organic framework ZIF-8 photocatalyst, and the another is FDH@ZIF-8 (enzyme catalyst) prepared by coupling ZIF-8 with FDH. The photocatalyst-enzyme system was constructed for the reduction of CO<sub>2</sub> to formic acid. A discussion on the experimental photocatalytic conversion of CO<sub>2</sub> under different

conditions was performed. The feasibility of the novel catalyst was verified through comparative experiments, including experiments without adding a photocatalyst, experiments without connecting PEI, experiments on repeatability without immobilization, and experiments with free enzymes. The results

showed that  $969.42 \mu\text{mol}\cdot\text{L}^{-1}$  of formic acid was generated by photocatalysis in the synthetic system, and the recovery rate still reached 71.05% after three cycles. The stability and durability have been significantly improved, enabling efficient capture of  $\text{CO}_2$  for the production of formic acid.



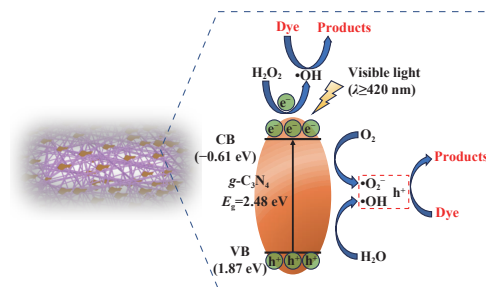
### Preparation of $g\text{-C}_3\text{N}_4/\text{PAN}+\text{TPU}$ Composite Nanofiber Membrane and Its Performance in Treating Organic Pollutants from Printing and Dyeing

ZHANG Han, WANG Libin, ZHANG Xia, ZHAO Ruiduo, HUANG Shushu

J. Mol. Catal. (China) **2025**, 39(2): 129–140.

Numerous significant issues have been brought to the water supply ecology by the quick rise of industrialization. Since traditional wastewater treatment techniques have several drawbacks, photocatalytic degradation has gained popularity as a straightforward and effective treatment method. Therefore, in order to generate materials with good filtration and catalytic capabilities in the treatment of printing and dyeing organic wastewater, a series of nanofiber membranes were made by electrospinning technology using PAN and TPU as carrier and  $g\text{-C}_3\text{N}_4$  as loading material. By adjusting the  $g\text{-C}_3\text{N}_4$  concentration, spinning voltage, and spinning liquid flow rate, the ideal spinning procedure was examined. The shape, structure, and

micro-size of nanofiber films are all influenced by distinct spinning processes, as demonstrated by the findings of scanning and Fourier transform infrared spectroscopy (FTIR) studies. The experimental findings demonstrated that the nanofiber membrane exhibited the highest visible light removal efficiency of 83.12% when subjected to the following parameters: 0.6%  $g\text{-C}_3\text{N}_4$  concentration, carrier PAN/TPU, spinning voltage 25 kV, and spinning liquid flow rate  $2.0 \text{ mL}\cdot\text{h}^{-1}$ . Simultaneously, mechanism investigations revealed that the primary active species in the catalytic elimination of reactive brilliant red were  $\text{h}^+$ ,  $\cdot\text{O}_2^-$ , and  $\cdot\text{OH}$ . In the realm of wastewater treatment, it offers a proposal for a photocatalytic membrane.



### Influence of Acidity and Pore Space Regulation of HZSM-5 Zeolite on Propane Aromatization Activity and Product Selectivity

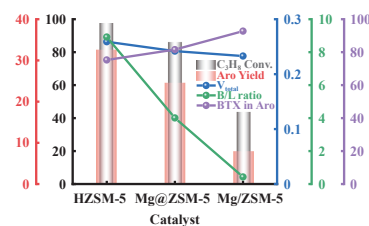
MA Yue, HUANG Lingxiang, TAN Yuhang, AN Haitao, ZHANG Qiang, ZENG Penghui, ZHU Xiaochun, SHEN Baojian

J. Mol. Catal. (China) **2025**, 39(2): 141–153.

The pore space and acidity of HZSM-5 were regulated by

using Mg, Mg@ZSM-5 and Mg/ZSM-5 samples were obtained by *in-situ* synthesis and incipient wetness impregnation methods respectively. The results indicate that different modification methods have a significant impact on their Mg distribution, acidity, and pore structure. After introducing Mg species through *in-situ* synthesis, the Mg species were uniformly distributed in the catalyst, the total acid, B and L acid content of Mg@ZSM-5 zeolite increased compared to unmodified HZSM-5, but the B/L value significantly decreased. The Mg/ZSM-5 sample prepared by impregnation method mainly has surface and shallow distribution of  $\text{MgO}$ , compared

with unmodified HZSM-5, it eliminates a large number of B acid sites and effectively increases the amount of L acid sites, while the overall acid content remains unchanged. It is found that the pore volume controls the BTX selectivity and the B/L ratio controls the propane conversion rate and temperature and the aromatization temperature.



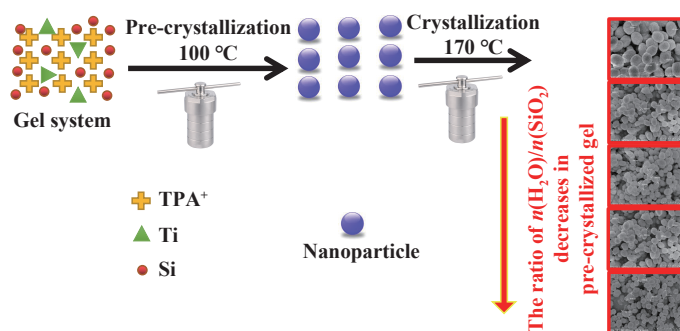
### Effect of Crystal Size of TS-1 Zeolite on 1-Hexene Epoxidation

REN Shenyong, ZHANG Min, CHEN Yao, ZHANG Yuqi, SHEN Baojian, XU Chunming

J. Mol. Catal. (China) **2025**, 39(2): 154–165.

Due to diffusion limitations within the pores of the catalysts, the epoxidation reaction of high carbon olefins often has lower activity. This article adopts the strategy of adding water and silicon source in the pre-crystallization solution to

synthesize small particle size TS-1 catalyst, while reducing the amount of template agent and ultimately reducing the synthesis cost. The catalytic diffusion pathway of the TS-1 with small particle size is significantly shortened, and an intergranular mesoporous structure is formed between its grains, which is conducive to the mass transfer of reactant molecules and greatly improves its catalytic performance for the epoxidation of high carbon olefins. The TS-1 exhibits good conversion rate and selectivity for the epoxidation of 1-hexene with  $\text{H}_2\text{O}_2$ . It was found that with the decrease of the ratio of  $n(\text{H}_2\text{O})/n(\text{SiO}_2)$  in the pre-crystallized gel and the increase of the pre-crystallization temperature, the size of TS-1 will decrease accordingly.



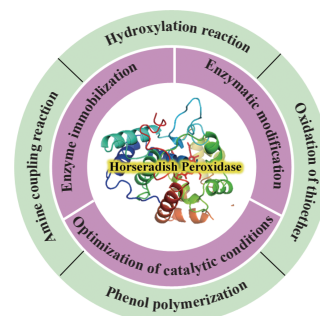
### Research Progress of Horseradish Peroxidase and Its Application in Organic Synthesis

HAN Xiaofeng, SU Lide, LI Na

J. Mol. Catal. (China) **2025**, 39(2): 166–177.

Horseradish peroxidase (HRP), an oxidase derived from the plant horseradish, exhibits extensive application potential in the field of organic synthesis as a versatile biocatalyst. Under the action of alkyl peroxides or hydrogen peroxide, it can efficiently catalyze a variety of complex organic reactions under mild conditions, demonstrating high catalytic activity and becoming an important tool in the field of green chemistry. Moreover, the catalytic mechanism of HRP is unique, not only featuring high reaction efficiency but also being environmentally friendly. It is consistent with the requirements of sustainable development. In this article, the multiple reaction types catalyzed by HRP are systematically summarized based on the

structure and catalytic properties. Furtherly, the key factors affecting the efficiency of catalytic reaction are discussed in detail. The corresponding optimization strategies are proposed in the article. Looking forward to the future, the application prospect of HRP in organic synthesis is broad, and it is expected to provide more green and efficient catalytic solutions for the research and development of new drug, materials science and other fields.



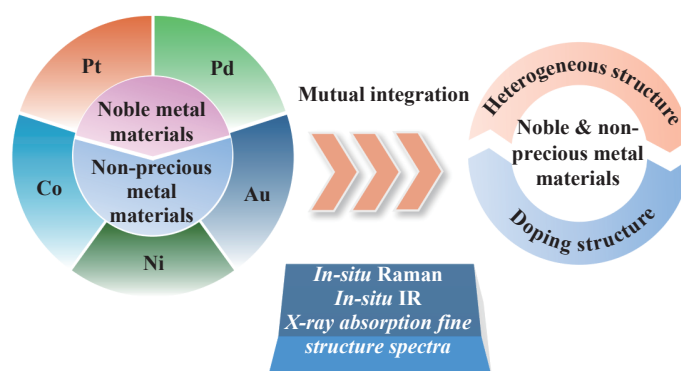
## Advances in Coupled Hydrogen Production from Alcohol Oxidation Catalyzed by Noble and Non-Precious Metal Materials

CAO Lijuan, ZHANG Rongxin, ZHOU Lei

J. Mol. Catal. (China) **2025**, 39(2): 178–187.

Transition metal catalysts play a key role in electrocatalytic alcohol oxidation coupled with hydrogen production. Therefore, it is of great significance to delve into the formulation and modification mechanism of both noble and non-precious transition metal catalysts. Related studies have been carried out on the catalysts modification strategies in terms of nanostructure optimization, electronic structure modulation, and

multicomponent synergistic effect, such as the noble metals Pt, Au, and Pd, the nonprecious transition metals Co and Ni, as well as the combinations of the noble metals and nonprecious transition metals in the form of doping and heterostructures. The mechanisms of heteroatom doping, vacancy engineering, alloying, core-shell structure and other strategies for microstructuring of alcohol oxidation electrocatalysts are reviewed in detail, and the significant effects of *d*-electron orbitals, vacancy orbitals and lattice parameters on the catalytic performance of the catalysts are analyzed in detail, followed by a schematic analysis of the typical characterization techniques, such as *in-situ* Raman, *in-situ* infrared, and X-ray absorption fine-structure spectroscopy. Finally, the microscopic regulation of catalysts is summarized, and its development prospects are envisioned, which is expected to achieve further breakthroughs in the field of electrocatalysis.



## Current Research Status and Progress of SO<sub>2</sub> Resistant Catalysts for Catalytic Combustion of Low-carbon Alkane VOCs

PENG Qian, DONG Fang, HAN Weiliang, HAN Weigao, TANG Zhicheng, ZHOU Zhifang

J. Mol. Catal. (China) **2025**, 39(2): 188–198.

Low-carbon alkane VOCs are difficult to eliminate due to their stable C—H bonds, which seriously affects the quality of the atmospheric environment and threatens human health. Catalytic combustion technology is widely used in the treatment of VOCs owing to the advantages of high destruction efficiency and few by-products. The core of the catalytic combustion method is the catalyst, which can be divided into noble metal and non-noble metal catalysts, and both of them are susceptible to the influence of SO<sub>2</sub> and lead to deactivation in practical applications. Specifically, SO<sub>2</sub> easily competes with VOCs molecules for active sites on the catalyst, which reduces the destruction efficiency and causes reversible deactivation; or even reacts with active components or supports to generate stable sulfates, which destroys the catalyst structure and causes

irreversible deactivation. In the existing studies, the anti-SO<sub>2</sub> poisoning strategies for catalysts of low-carbon alkane VOCs catalytic combustion mainly include the construction of double noble metal catalytic system, elemental doping, acidification treatment, and the construction of core-shell structure catalysts, etc. Among them, the construction of dual noble metal catalytic system and the construction of core-shell structure catalyst can inhibit the interaction of SO<sub>2</sub> with the active phase from the source, which is more effective for noble metal catalysts. In contrast, active phases of non-noble metal catalysts are usually very dispersed, and it is more effective to enhance SO<sub>2</sub> resistance by doping elements.

